Journal of Materials Chemistry C

Accepted Manuscript

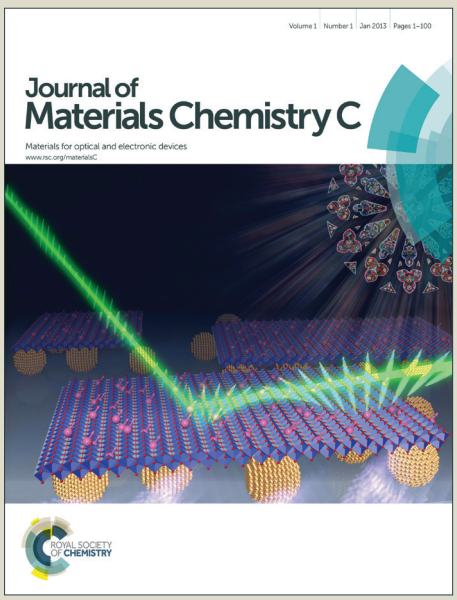

ROYAL SOCIETY OF CHEMISTRY

www.rsc.org/materialsC

ToC

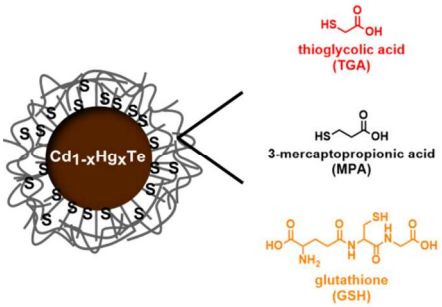

Influence of different thiol ligands on growth kinetics, photoluminescence quantum yields, and colloidal stability of near-infrared emitting CdHgTe nanocrystals is systematsically studied.

Journal of Materials Chemistry C

RSCPublishing

ARTICLE

Influence of the stabilizing ligand on the quality, signal-relevant optical properties, and stability of near-infrared emitting $Cd_{1-x}Hg_xTe$ nanocrystals

Cite this: DOI: 10.1039/x0xx00000x

Received 00th xxx 2014,
Accepted 00th xxx 2014

DOI: 10.1039/x0xx00000x

www.rsc.org/

S. Leubner[a], R. Schneider[b], A. Dubavik[a], S. Hatami[b], N. Gaponik[a*], U. Resch-Genger[b*] and A. Eychmüller[a]

Bright and stable near-infrared (NIR) and infrared (IR) emitting chromophores are in high demand for applications in telecommunication, solar cells, security barcodes, and as fluorescent reporters in bioimaging studies. The best choice for wavelengths > 750 nm are semiconductor nanocrystals, especially ternary or alloy nanocrystals like CdHgTe, which enable size and composition control of their optical properties. Here, we report on the influence of growth time and surface chemistry on the composition and optical properties of colloidal CdHgTe. Up to now, these are the only NIR and IR emissive quantum dots, which can be synthesized in high quality in water, using a simple one-pot reaction. For this study we utilized and compared three different thiol ligands, thioglycolic acid (TGA), 3-mercaptopropionic acid (MPA), and glutathione (GSH). Aiming at the rational design of bright NIR- and IR-emissive alloy materials, special emphasis was dedicated to a better understanding of the role of the surface ligand and adsorption-desorption equilibria on the photoluminescence quantum yield and stability. In this respect, dilution and protonation studies were performed. Our results show that with this simple synthetic procedure, strongly fluorescent CdHgTe colloids can be obtained with MPA as stabilizing ligand revealing quantum yields as high as 45 % independent of particle concentration.

Introduction

There is an ever increasing interest in bright and stable NIR and IR emitting chromophores that can be used for a variety of applications ranging from solar cells,[1] fluorescent reporters for bioimaging,[2,3] security barcodes,[4,5] and active materials for telecommunication.[6] For wavelengths > 750 nm, organic dyes are only of very limited use as they possess small QY values in the order of maximum 0.20 in organic solvents[7] and 0.04 in water in the wavelength region of 750 to 950 nm[8,9] and for wavelengths > 1000 nm even < 0.002.[10] Additionally disadvantageous are their limited thermal and photochemical stability. For some applications like fluorescence lifetime imaging increasingly used for *in vitro* and *in vivo* imaging studies e.g., to improve signal-to-noise or background ratios, their short emission lifetimes (typically < 2 ns) can hamper their successful use for time-gated emission and lifetime discrimination.[11–14] Far more ideal systems present semiconductor nanocrystals (NCs) with NIR and IR emission, which show size-tunable absorption and emission bands, thereby enabling the coverage of a broad wavelength region via size and, in the case of alloy materials, also via material composition. Additionally, they enable the free choice of photoluminescence (PL) excitation wavelength perfect for spectral multiplexing[11,15] and possess unbeatably high photoluminescence quantum yields (PL QYs). A comprehensive review on narrow bandgap semiconductor NCs has recently been published by the group of Rogach.[15] The most popular representatives are lead chalcogenides, which are usually prepared in organic solvents, and require either ligand exchange or encapsulation for use in water.[16–18] The only colloids that can be presently synthesized in sufficient quality directly in water are CdHgTe nanocrystals. This, in conjunction with the possibility to tune the optical properties not only by size, yet also by material composition, renders these materials very attractive for all applications in aqueous environments[15,19,20] and for applications imposing size restrictions or requiring reporters of identical size, but with different optical properties.

A major challenge for nanoparticle systems presents the control of their photoluminescence under application-relevant conditions, especially for nanocrystal systems with non-covalently attached ligands prone to ligand adsorption-desorption equilibria. Ligands, also known as stabilizers, provide control of the nucleation and growth kinetics, passivate the NC surface by electronic interaction with surface sites, and provide stability, solubility, and functionality.[21] Frequently employed ligands for Cd-based NCs are thiols, as they can passivate electron trap states and thereby increase the PL QY.[22] However, until now, the lack of a complete understanding of

the influence of the NC surface chemistry on their PL and its control hampers the routine application of these fascinating materials. This includes also the concentration dependence of the PL QY as many applications like cellular imaging studies or the incorporation of nanocrystals into polymeric beads or inorganic matrices typically involve dilution steps.[23,24] For example, we recently showed for CdTe NCs that their PL QY decreases with dilution of the parent colloid in a size- and surface shell-specific manner.[25,26] Moreover, ligand desorption-related changes in PL QY can correlate with a reduced stability of the NC, possibly resulting in the release of toxic metal ions or anions.[27] Hence, surface functionalization strategies are desired, which can circumvent such effects utilizing e.g., multivalent ligands[23] or encapsulation strategies relying on amphiphilic polymers that can be cross-linked.[28,29] The latter, however, leads to a considerable increase in NC size, which is disadvantageous for all applications with size restrictions like energy transfer-based signaling strategies and cellular imaging.
This encouraged us to extend our previously reported studies of CdTe colloids[26] to more complex alloy CdHgTe NCs. Here, the PL is influenced by the size and the composition of the NC core, i.e., the Hg-to-Cd ratio and the different stages of mercury penetration into the CdTe crystal as well as the shape, crystal structure,[30] and surface chemistry. The latter includes the type of ligand and its binding strength to the surface atoms, the ligand density, and the shell composition. For carboxylated thiols, also the pH can strongly influence the stability and optical properties by the control of chemical nature and electron density of the ligand, as it was shown for CdTe NCs.[31–33]
In this respect, based on the recently reported simple one-pot reaction approach of Lesnyak et al. to the aqueous synthesis of CdHgTe,[20] we prepared CdHgTe NCs with three thiol ligands, i.e., thioglycolic acid (TGA), 3-mercaptopropionic acid (MPA), and glutathione (GSH), respectively. We subsequently assessed the influence of the ligand on the growth kinetics and the optical properties of the resulting colloids. TGA and MPA were chosen as these ligands yield the highest PL QY for CdTe NCs[34] and GSH can be advantageous to improve the compatibility with biological media. Special emphasis is dedicated to the influence of the surface ligand on PL QY, NC stability, and to the influence of pH, thereby paving the road to achieve synthetic control of the surface chemistry of NCs. This may enable the rational design of bright and stable NIR and IR emissive NCs for a broad range of applications.

Experimental

Materials

All chemicals used for the synthesis of the CdHgTe NCs were of analytical grade or of the highest purity available and employed without additional purification. In detail, $Cd(ClO_4)_2$•$6H_2O$ (Alfa Aesar), $Hg(ClO_4)_2$•$6H_2O$ (Alfa Aesar), NaOH (Sigma-Aldrich), Al_2Te_3 (Cerac Inc.), H_2SO_4 (Sigma-Aldrich), 2-propanol (Merck), TGA (Merck), MPA (Aldrich), and GSH (Sigma-Aldrich) were used. All solutions were prepared using Milli-Q water (Millipore) as the solvent. The quantum yield standards IR125 (batch number 10970) and Nile Red (batch number 333298/1 1196) were obtained from Lambda Physik and Fluka. The organic solvent used for the preparation of the QY standard solution, i.e., dimethyl sulfoxide (DMSO) was of spectroscopic grade and purchased from Sigma-Aldrich. For the Ellman's test and pD experiments 5,5'-dithiobis(2-nitrobenzoic acid) (DTNB, Aldrich), NaH_2PO_4 (Sigma-Aldrich), ethylenediaminetetraacetic acid (EDTA, Sigma), Na_3PO_4 (Aldrich), and DCl (Aldrich) were used.

Synthesis of thiol-capped CdHgTe NCs

CdHgTe NCs were synthesized according to the procedure published elsewhere.[20] For all samples the initial molar ratio of Cd^{2+} : Hg^{2+} : Te^{2-} : thiol was set to 0.95 : 0.05 : 0.75 : 1.3. In a three-necked flask fitted with a septa and valves, $Cd(ClO_4)_2 \cdot 6H_2O$ and $Hg(ClO_4)_2 \cdot 6H_2O$ were dissolved in 250 ml of water and either thioglycolic acid (TGA), 3-mercaptopropionic acid (MPA) or glutathione (GSH) was added under stirring, followed by adjusting the pH to 12 by dropwise addition of a 1 M NaOH solution. The solution was deaerated by bubbling with argon for 1 h. H_2Te gas, which was generated by the reaction of Al_2Te_3 lumps with an excess amount of 0.5 M H_2SO_4, was passed through the solution for ca. 30 min together with a slow argon flow under stirring. Formation and growth of the NCs proceeded upon reflux. The samples were concentrated on a rotary evaporator, precipitated by addition of 2-propanol and subsequently dissolved in water. No special treatments to control and reduce the size distribution or to increase PL QY were applied post-preparatively.
Additionally to the three ligands presented, bidentate dihydrolipoic acid (DHLA) was applied for the CdHgTe NC synthesis. This molecule equipped with two thiol groups was thought to introduce stronger surface binding as shown e.g., for CdSe colloids.[35] Unfortunately, with this promising ligand,[36] we could not obtain stable CdHgTe NCs under conditions allowing comparative studies with the other monodentate thiols. That is why solely NCs stabilized with TGA, MPA, and GSH are discussed below.

Methods

Characterization of the NCs. Samples for transmission electron microscopy (TEM) were prepared by rinsing a copper grid coated with a silicon dioxide film with diluted NC solutions and subsequently evaporating the solvent. TEM imaging was carried out on a Tecnai F20 microscope (from FEI Company), operating at 200 kV acceleration voltage.
The elemental analysis was done on a Perkin Elmer Optima 7000DV ICP-OES system with an instrumental error below 1 %. Cd quantification was performed at 214.44 nm and 228.80 nm and Hg quantification at 194.17 nm and 253.65 nm. For S detection wavelengths of 180.67 nm and 181.975 nm and for Te 214.28 nm were used. All results were obtained from triple measurements with relative standard deviations below 3 % for Cd, below 10 % for Hg, below 14 % for S and below 1 % for Te.
Optical spectroscopy. All samples were diluted with D_2O due to absorption of H_2O in the NIR spectral region at 910 nm, thereby minimizing solvent influences on the photophysical studies. The pD of the diluted solutions was adjusted to that of the QD stock solution subsequently by addition of NaOD.
UV/Vis absorption spectra were recorded with a calibrated Cary 5000 spectrophotometer (Varian Inc., Palo Alto, USA). Fluorescence and PL QY measurements were performed with a Fluorolog-3 spectrofluorometer (HORIBA Jobin Yvon Inc., Edison, NJ, USA) at TUD and a calibrated FSP-920 fluorometer (Edinburgh Photonics) at BAM. Additional fluorescence studies with special emphasis to the measurement of corrected emission spectra (relative to the spectral radiance scale) and the relative determination of PL QY were done with a calibrated FSP-920 fluorometer (Edinburgh Instruments) at

BAM equipped with a Xe lamp, Czerny-Turner double monochromators, a reference channel, and Glan-Thompson polarizers placed in the excitation and emission channels set to 0° and 54.7°, respectively (magic angle conditions) to render detected emission intensities independent of possible emission anisotropies.[37,38] The relative determination of PL QY from the absorption and corrected emission spectra (blank and spectral correction) of the sample and standard in air-saturated solution was performed according to Ref 25. We used the quantum yield standards IR125 (excitation wavelength: 808 nm; solvent DMSO; PL QY = 0.228)[7] and Nile Red (excitation wavelength: 550 nm; solvent ethanol; PL QY = 0.64)[39] for the emission region of 825 to 1200 nm utilizing IR 125 to analyze sample T and M and 700 to 1100 nm employing Nile Red for analysis of sample G. All absorption and fluorescence measurements were performed with air-saturated freshly prepared NC or dye solutions at T = (25 +/- 1) °C using 10 mm × 10 mm quartz cuvettes from Hellma GmbH. The absorbance of the NC and dye solutions used for the relative determination of PL QY were within the range of 0.02 to 0.1 (at the first excitonic absorption maximum of the NC or the longest wavelength absorption maximum of the organic dye used as QY standard).

Ellman's test. Quantification of the number of thiol ligands per QD was performed by the Ellman's test.[40]A 3.4 mM stock solution of DTNB (Ellman's reagent) was freshly prepared in 0.15 M phosphate buffer (NaH_2PO_4) containing 1 mM EDTA (pH 8.2, adjusted with NaOH). Addition of EDTA to CdHgTe leads to the complete dissolution of the colloid as controlled by absorption and fluorescence measurements, revealing the absence of semiconductor NCs. For calibration, for each ligand a freshly prepared aqueous standard solution of the pure ligand (3 mM) was used. For this assay, 2900-2949 µl of buffer, 50 µl of Ellman's reagent solution, and 1-50 µl of the sample or calibration solution were mixed. The thiol concentration was determined after complete reaction by comparison of the absorbance at 412 nm with the calibration curves obtained for the pure ligand. To monitor the reaction process, absorption spectra were recorded in intervals of 5 or 10 minutes until no further changes in absorption were observed.

Dilution studies. Different volumes of the QD stock solutions were diluted with a NaOD solution previously adjusted to the pD of the stock solution. The resulting absorption spectra were measured in 10 mm quartz cuvettes and for extreme diluted solutions in 50 mm quartz cuvettes. The emission spectra were always measured in 10 mm quartz cuvettes.

Precipitation experiments. 900 µl of iso-propanol were added to 100 µl of the aqueous QD stock solution. The mixture was centrifuged and the clear supernatant was disposed. The precipitate was completely redispersed in NaOD solution.

pD experiments. A hydrogen free phosphate buffer (0.05 M Na_3PO_4) in D_2O was adjusted to five different pD values with DCl. For each pD value, a fresh sample was prepared by dilution of the same amount of the aqueous QD stock solution. The absorption and emission spectra were subsequently recorded. The pD value was checked after the measurement again. In general, the pD is the analog of the pH in D_2O solutions, but differs in value due to the different equilibrium constants of H_2O and D_2O. It is determined from standard measurements with a glass electrode in D_2O solutions according to the following equation:[41]

$$pD = pH_{reading} + 0.40$$

Results and discussion

Synthesis of differently stabilized CdHgTe NCs

The synthesis of CdHgTe NCs according to Lesnyak et al.[20] is very versatile and suitable for different thiol ligands as shown by us here for TGA, MPA, and GSH, see Figure 1, that present three of the most popular stabilizers used for CdTe NCs. All synthetic key parameters such as temperature, initial molar ratios of Cd, Hg, Te, and thiol, reaction volume, and pH were kept constant to ensure identical growth conditions. However, the use of different ligands causes variations in growth mechanisms. Therefore, it is not possible to synthesize samples with different stabilizers that have exactly the same size and composition after a constant growth time. For ternary systems, many parameters influence the optical properties of the resulting material, which makes a proper comparison of differently prepared, i.e., here differently stabilized, colloids very challenging. Hence, to minimize the number of variables and to allow a proper comparison, for each ligand, a set of samples was prepared with the aim to obtain samples with similar photoluminescence features.

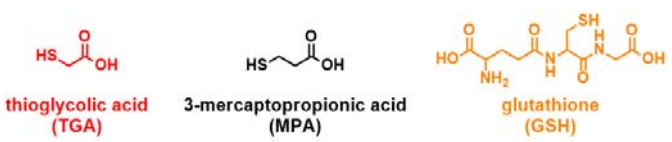

Figure 1 Chemical structures of the ligands used.

Comparison of cation-thiol binding strength

In Figure 2, the evolution of the emission maxima with reaction time is compared for the three different ligands. As for CdHgTe NCs not only the growth in size, but also the incorporation of mercury has an impact on the emission maximum, the kinetics are different compared to those observed for CdTe colloids.[21] Here, TGA-capped CdHgTe NCs give the fastest shift to long emission wavelengths. MPA-capped CdHgTe NCs can reach similar red emission maxima, although after a longer reaction time. However, complexes formed by mercury and GSH are so stable that the growth of NCs from Hg-GSH monomers is strongly slowed down and a limit of incorporation of mercury seems to be reached. Even after long reaction times, no NCs with emission maxima exceeding 850 nm could be obtained, yet the samples became unstable and aggregated.

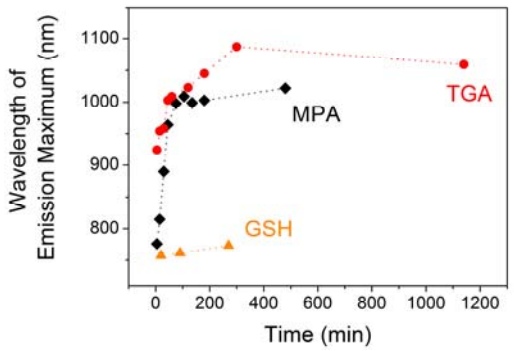

Figure 2 Evolution of the emission maxima with reaction time.

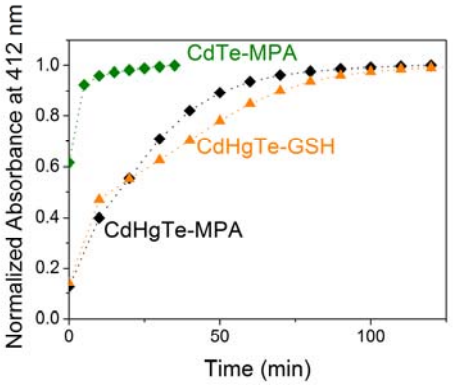

Figure 3 The temporal evolution of the absorption maximum at 412 nm during the quantification of thiols using Ellman's test reflects the strength of the NC-ligand bond.

The differences in the growth kinetics can be caused by the different complexation constants of the respective stabilizing thiols and Cd^{2+} and Hg^{2+}. For example, with 11.02 the log K value of $Cd^{2+}(GSH)^{3-}$ is significantly smaller than that of $Hg^{2+}(GSH)^{3-}$ reaching 27.36, which underlines the strong binding of GSH and mercury.[42,43] To further emphasize such effects, we performed Ellman's studies with these differently stabilized CdHgTe colloids. Similar studies have been previously reported by us for TGA-capped CdTe,[26] which were also used for comparison with the behavior observed for the CdHgTe series. During the colorimetric test, the NCs dissolve in the presence of EDTA and Ellman's reagent and release all thiol ligands, which are then quantified photometrically by the reaction with the Ellman's reagent yielding a yellow colored molecule with an absorption maximum at 412 nm. The process of dissolution and reaction with the analyte, i.e., the evolution of the complete absorption at 412 nm, takes a certain time and can be used to compare the influence of the Hg-ligand and Cd-ligand binding constants on the reaction kinetics for CdTe, CdHgTe and the three thiols. The results from the Ellman's studies are displayed in Figure 3.

A comparison of CdTe and CdHgTe stabilized by MPA reveals slower kinetics for CdHgTe. The slower formation of the product of the reaction of MPA and Ellman's reagent reflects the stronger binding of MPA to CdHgTe compared to CdTe due to the presence of Hg(II) ions. Similar effects were observed for the other thiols. There was no sign for the presence of two distinguishable particle-ligand bonds (Cd-thiol and Hg-thiol) in the CdHgTe particles, as the reaction progress is not directly related to the Hg content measured by ICP-OES. Screening experiments also showed that Hg-thiol complexes alone are not the reason for the different kinetics, as addition of $Hg(ClO_4)_2$ to CdTe particles lead to completely different spectra and kinetics of the Ellman's reaction than for CdHgTe. This implies that the overall strength of the NC-ligand bond is greater for CdHgTe. Slower kinetics observed for GSH-capped CdHgTe NCs compared to MPA point to a stronger binding of GSH to CdHgTe compared to MPA.

Characterization of the CdHgTe NCs

The CdHgTe samples were characterized by transmission electron microscopy (TEM), elemental analysis, and optical spectroscopy. As already mentioned, for ternary systems such as CdHgTe it is very challenging to obtain samples that provide reasonable comparability as their emission properties depend on one hand on the size and the core structure, i.e., the Cd-to-Hg ratio and incorporation of Hg^{2+}, and on the other hand on the chemical composition of the surface, i.e., the type and density of the capping agent and the chemical structure of the ligand shell and the surface atoms. Moreover, aqueous synthesis in presence of thiols usually results in a sulfur-enriched surface shell influencing the stability and PL of the nanocrystals.[21,44] The formation of this shell is a result of the hydrolysis of thiols employed and is usually thiol-dependent.[45] Taking this into account, we decided to perform a comparison based on the stage of growth of the different CdHgTe NCs, as this parameter is known to be directly related to their quality and their PL QY.[46,47] Figure 2 depicts the typical kinetics for the evolution of the position of the emission maximum of CdHgTe NCs. The samples at the beginning of the growth plateau are expected to be well comparable due to the completed phase of a pronounced change in PL and the accomplished growth. Thus, we chose the samples after the first strong rise in emission wavelength for further comparison. The samples investigated in the following are sample T, TGA-capped CdHgTe NCs taken after a reaction time of 45 min, M, MPA-capped CdHgTe NCs after 75 min, and G, GSH-capped CdHgTe NCs after 270 min, respectively (see Table 1 and Figure 4). TEM analyses reveal different sizes of the CdHgTe NCs, with the largest sizes resulting for the GSH-capped NCs. Representative images are shown in Figure 4 (left panel) and size histograms can be found in the Supporting Information (SI). Elemental analysis by ICP-OES, displayed in Table 1, yields different Hg contents with a lower Hg content observed for larger NCs.

One explanation can be here that Hg is preferentially incorporated into the particles during the initial stage of seed formation due to lower solubility of HgTe than CdTe in water. In this case, particle growth at later stages proceeds through incorporation of mainly cadmium ions. Additional effects influencing the Hg content may origin from the different cation-thiol binding strengths leading to an enhanced Hg incorporation for TGA-capped CdHgTe NCs compared to GSH, for which the release of Hg monomers is slowed down due to the greater stability of cation-thiol complexes. Nevertheless, for MPA- and TGA-capped NCs, these differences in size and composition result in NCs with similar absorption maxima. The different Te content results from the varied growth times and consequently, the different times for Te oxidation. Moreover, the Te content of all samples is relatively small. This could imply that a certain amount of sulfur is incorporated into the NCs and also, that Cd^{2+} and Hg^{2+} ions are part of the ligand shell coordinated by thiolates.

Table 1 Characteristics of the different capped CdHgTe NCs.

	CdHgTe-TGAT	CdHgTe-MPAM	CdHgTe-GSHG
growth time	45 min	75 min	270 min
$\lambda_{1s\text{-}1s,max}$	864 nm	880 nm	730 nm
$\lambda_{em,max}$	1046 nm	973 nm	770 nm
size	4.2 ± 1.3 nm	5.0 ± 1.2 nm	5.8 ± 1.7 nm
quantum yield	0.20	0.45	0.14
elemental composition	Cd : Hg : Te : S = 0.976 : 0.024 : 0.351 : 1.34	Cd : Hg : Te : S = 0.992 : 0.008 : 0.149 : 0.96	Cd : Hg : Te : S = 0.995 : 0.005 : 0.060 : 1.19

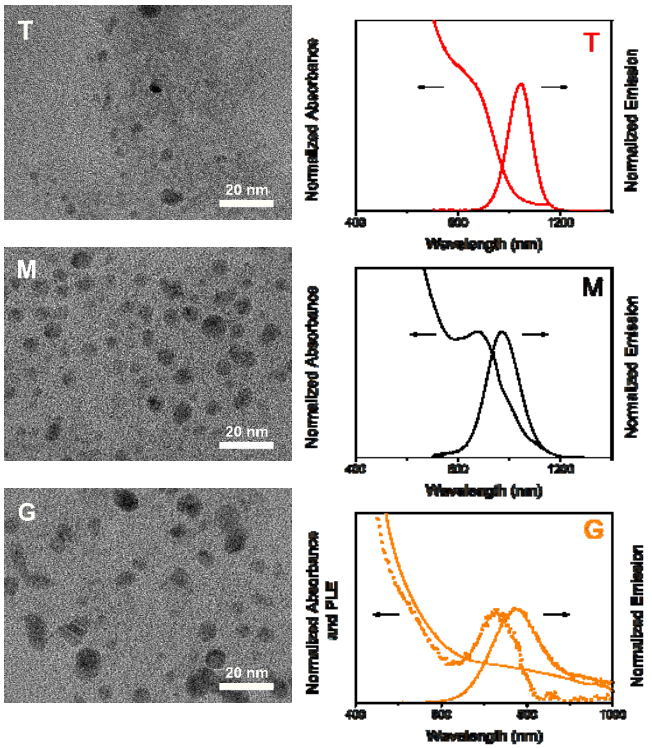

Figure 4 Left: TEM pictures. Right: Absorption and emission features of selected TGA-(T, upper part, red), MPA-(M, middle part, black), and GSH-capped CdHgTe NCs (G, lower part, orange). For GSH-capped NCs the PL excitation spectrum (dotted line) shows a maximum, which is not visible in the absorption features (solid line).

Similar results were observed and deeply investigated in the case of equally stabilized CdTe NCs.[21,26,44] The value for the sulfur content in Table 1 includes besides the sulfur content of the NC core also the contribution from all ligands present at the NC surface and free in solution.

Figure 4 shows the absorption and emission spectra of the samples T and M, CdHgTe-TGA (upper part, red) and CdHgTe-MPA (middle part, black), respectively. Notably, the absorption maxima are located at rather similar wavelengths, i.e., at 864 nm and 880 nm, respectively. Nevertheless, the emission maxima peak at 1046 nm and 973 nm, respectively and hence, the Stokes shifts differ by a factor of two for T and M. This implies that TGA and MPA lead to different surface passivation causing a varied electronic structure of the NC.

As it follows from Figure 4 (lower part, orange) summarizing the absorption, emission and PL excitation spectrum of sample G, the absorption spectrum of GSH-capped CdHgTe NCs shows no distinct features and extends to longer wavelengths. This can point to the formation of bigger NCs in conjunction with a broader size distribution. Comparison of the absorption and PL excitation spectra recorded at the emission maximum revealed that the latter shows the expected maximum at 730 nm and the species absorbing at higher wavelength are non-emissive. For GSH-capped CdHgTe NCs, it was not possible to obtain NCs with emission maxima reaching 1000 nm. Importantly, also the PL QYs differ for the three samples. MPA-capped CdHgTe NCs reveal a promisingly high PL QY of 45 %, which is superior to any NIR emitting organic dye and among the highest PL QY values reported for such NCs in water.[6,20,48] Nevertheless, with a PL QY of 20 % TGA-capped CdHgTe NCs are also more emissive than organic dyes emitting in the same spectral region.

Influence of NC concentration on PL QY

Aiming at the use of these CdHgTe NCs as fluorescent reporters for bioimaging studies, we studied the influence of the NC environment, i.e., NC concentration and pH on the PL QY and the stability of the colloids. Previous studies with TGA-stabilized CdTe colloids of different size show a size-dependent and strong decrease of the PL QY at low NC concentration due to dilution-induced ligand desorption processes, which is disadvantageous for e.g., bioimaging. In contrast, the investigated CdHgTe NCs do not show a concentration dependence of their PL QY (see Figure 5). This, in conjunction with their red emission maxima, high PL QY, and ease of preparation renders these CdHgTe systems especially attractive as new generation of fluorescent reporters. Even additional precipitation of the MPA-capped CdHgTe sample with iso-propanol, a non-solvent, which decreases the amount of ligands on the surface of the NC, does not cause a clear concentration dependence of the PL QY. This suggests that the ligand shell is very stable. One reason could be that the stabilizing ligands are very tightly bound to the CdHgTe core and hence not subject to ligand adsorption-desorption equilibria any more. This finding emphasizes also the favorable influence of even small amounts of Hg^{2+} on the optical properties and stability of such alloy NCs.

Also, the large amount of sulfur present in the NCs assists the observed good stability. Our previous study on CdTe could show that larger NCs are subject to a weaker concentration dependence than smaller NCs.[25] As the size of the CdTe NC correlates with the sulfur content due to the hydrolysis of thiols,[45] a highly sulfur enriched shell at the NC surface may also be a reason for a strong emission independent on the NC concentration. A similar behavior may be also true for CdHgTe, meaning that the presence of sulfur supports the high PL and the stability upon dilution. Alternatively, the solvent D_2O, forming less strong "hydrogen" bonds than water, possibly influences the bonding of the thiol ligands and the NC surface, although we tentatively favor the former explanations.

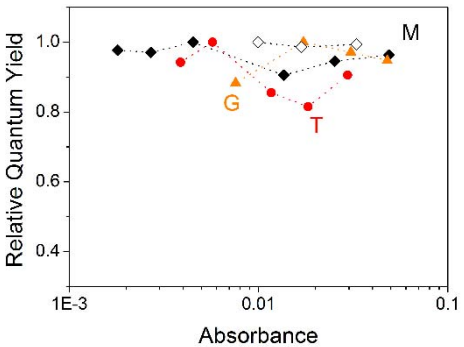

Figure 5 Promisingly, the PL QY of all CdHgTe NC samples does not show a concentration dependence for the stock solutions (filled symbols) and after additional precipitation of sample M (open symbols). The absorbance is used here as measure for NC concentration. Precipitation leads to the removal of free ligand and also ligand from the NC surface. The PL QY was normalized to the value for the highest concentration for better comparability. The dotted lines are only a guide to the eye.

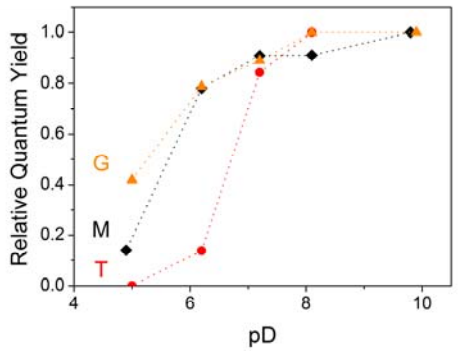

Figure 6 Dependence of PL QY on pD. The dotted lines are only a guide to the eye. The values are normalized to the respective PL QY at pD = 10 for better comparison.

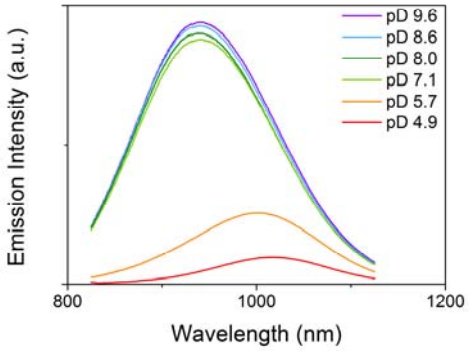

Figure 7 Changes of the emission spectra of sample M (CdHgTe-MPA) upon variation of pD.

Influence of pD on PL QY

The suitability of the ligands for surface stabilization of CdHgTe was additionally evaluated by the comparison of pH-dependent changes of the absorption and emission features. In Figure 6, the changes of the PL QY with variation of pD, the value that is considered here analog to the pH value in D_2O solution, are depicted for T, M, and G. The values are normalized to the PL QY at pD = 10 for better comparison. In general, the behavior is similar for all three ligands, which is a decrease of the PL QY at pD values smaller than 7. For TGA-capped CdHgTe the emission is completely quenched at pD = 5 and strongly diminished for MPA-capped CdHgTe. The smallest changes occur for GSH, as a slighter pD dependence is expected from the presence of both amino and acid groups.
Figure 7 shows the spectral changes of the emission upon variation of the pD for sample M. By decreasing the pD to values below 7, the emission intensity decreases strongly concomitantly with a shift of the emission maximum to longer wavelengths. Additionally, the FWHM decreases at pD values below 7. This observation suggests the precipitation of small NCs at lower pD, which is reasonable as due to the larger surface-to-volume ratio for smaller NCs changes of the surface chemistry effect their stability to a greater extend. Changes at the NC surface may include protonation of the thiol ligand and consequent desorption from the NC surface leaving behind a destabilized ligand shell and surface traps. Absorption measurements indicate colloidally stable NCs at pD values higher than 5.7, whereas for smaller pD values, scattering becomes clearly visible indicating the onset of particle aggregation. This supports the thesis that certain NCs become instable and precipitate. A similar behavior can also be observed for the other samples as well as for CdTe NCs.

Conclusions

In summary, we have presented a simple one pot synthesis of CdHgTe NC using three different monodentate thiol ligands TGA, MPA, and GSH. This enables tuning of the emission of CdHgTe and its extension into the NIR even for small NCs with the aid of ligand-dependent growth mechanisms. Moreover, the ligand seems to crucially affect the photoluminescence quantum yields (PL QY) of the resulting alloy NCs. Altogether, TGA is a suitable ligand for moderately emissive CdHgTe NCs with long wavelength emission up to 1100 nm, MPA yields highly emissive CdHgTe NCs with PL QYs as high as 45 %, yet slightly shorter emission maxima, and GSH is promising for applications in biological systems, even though only for NCs with an emission up to 800 nm. Moreover, contrary to their CdTe counterparts, the CdHgTe NCs reveal concentration-independent PL QY. Thus the absence of ligand adsorption-desorption equilibria, typically undesired for the use of nanocrystals as fluorescent reporters, underlines the beneficial influence of mercury doping. In this respect, this work contributes to the goal of producing design criteria for highly NIR and IR emissive and long-term stable NCs and the derivatization of structure-property relationships.

Acknowledgements

This work was supported by the German Research Foundation (DFG) projects EY16/14-1 and RE1203/12-1 and within the Cluster of Excellence ‘Center for Advancing Electronics Dresden’. We thank Christine Damm (IFW Dresden e.V.) for assistance in performing the TEM imaging and Renate Schulze (TU Dresden) for ICP-OES analyses.

Notes and references

[a] Physical Chemistry and Center for Advancing Electronics Dresden, TU Dresden, Bergstr. 66b, 01062 Dresden, Germany
[b] BAM Federal Institute for Materials Research and Testing, Richard-Willstätter-Str. 11, 12489 Berlin, Germany
* Corresponding Author
nikolai.gaponik@chemie.tu-dresden.de
ute.resch@bam.de
Electronic Supplementary Information (ESI) available: TEM histograms. See DOI: 10.1039/b000000x/

1. H. Wei, H. Zhang, H. Sun, W. Yu, Y. Liu, Z. Chen, L. Cui, W. Tian, and B. Yang, *J. Mater. Chem.*, 2012, **22**, 17827–17832.

2. Y. Wang, C. Ye, L. Wu, and Y. Hu, *J. Pharm. Biomed. Anal.*, 2010, **53**, 235–242.

3. J. Frangioni, *Curr. Opin. Chem. Biol.*, 2003, **7**, 626–634.

4. S. Fournier-Bidoz, T. L. Jennings, J. M. Klostranec, W. Fung, A. Rhee, D. Li, and W. C. W. Chan, *Angew. Chem.*, 2008, **120**, 5659–5663.

5. M. Han, X. Gao, J. Z. Su, and S. Nie, *Nat. Biotechnol.*, 2001, **19**, 631–635.

6. M. Harrison, S. Kershaw, and M. Burt, *Pure Appl. Chem.*, 2000, **72**, 295–307.

7. C. Würth, J. Pauli, C. Lochmann, M. Spieles, and U. Resch-Genger, *Anal. Chem.*, 2012, **84**, 1345–1352.

8. S. A. Soper and Q. L. Mattingly, *J. Am. Chem. Soc.*, 1994, **116**, 3744–3752.

9. J. Pauli, T. Vag, R. Haag, M. Spieles, M. Wenzel, W. A. Kaiser, U. Resch-Genger, and I. Hilger, *Eur. J. Med. Chem.*, 2009, **44**, 3496–3503.

10. S. Hatami, C. Würth, S. Leubner, M. Kaiser, S. Gabriel, V. Lesnyak, N. Gaponik, A. Eychmüller, and U. Resch-Genger, *In Preparation*.

11. U. Resch-Genger, M. Grabolle, S. Cavaliere-Jaricot, R. Nitschke, and T. Nann, *Nat. Methods*, 2008, **5**, 763–775.

12. M. Y. Berezin and S. Achilefu, *Chem. Rev.*, 2010, **110**, 2641–2684.

13. J. E. Mathejczyk, J. Pauli, C. Dullin, J. Napp, L.-F. Tietze, H. Kessler, U. Resch-Genger, and F. Alves, *Mol. Imaging*, 2011, **10**, 469–480.

14. R. Tang, H. Lee, and S. Achilefu, *J. Am. Chem. Soc.*, 2012, **134**, 4545–4548.

15. S. V. Kershaw, A. S. Susha, and A. L. Rogach, *Chem. Soc. Rev.*, 2013, **42**, 3033–3087.

16. A. L. Rogach, A. Eychmüller, S. G. Hickey, and S. V. Kershaw, *Small*, 2007, **3**, 536–557.

17. E. H. Sargent, *Adv. Mater.*, 2005, **17**, 515–522.

18. S. G. Hickey, N. Gaponik, and A. Eychmüller, *Photonics Nanostructures - Fundam. Appl.*, 2007, **5**, 113–118.

19. S. Gupta, O. Zhovtiuk, A. Vaneski, Y.-C. Lin, W.-C. Chou, S. V. Kershaw, and A. L. Rogach, *Part. Part. Syst. Charact.*, 2013, **30**, 346–354.

20. V. Lesnyak, A. Lutich, N. Gaponik, M. Grabolle, A. Plotnikov, U. Resch-Genger, and A. Eychmüller, *J. Mater. Chem.*, 2009, **19**, 9147–9152.

21. A. L. Rogach, T. Franzl, T. A. Klar, J. Feldmann, N. Gaponik, V. Lesnyak, A. Shavel, A. Eychmüller, Y. P. Rakovich, and J. F. Donegan, *J. Phys. Chem. C*, 2007, **111**, 14628–14637.

22. S. Jeong, M. Achermann, J. Nanda, S. Ivanov, V. I. Klimov, and J. A. Hollingsworth, *J. Am. Chem. Soc.*, 2005, **127**, 10126–10127.

23. J. B. Delehanty, K. Susumu, R. L. Manthe, W. R. Algar, and I. L. Medintz, *Anal. Chim. Acta*, 2012, **750**, 63–81.

24. C. Dong and J. Irudayaraj, *J. Phys. Chem.*, 2012, **116**, 12125–12132.

25. M. Grabolle, M. Spieles, V. Lesnyak, N. Gaponik, A. Eychmüller, and U. Resch-Genger, *Anal. Chem.*, 2009, **81**, 6285–6294.

26. S. Leubner, S. Hatami, N. Esendemir, T. Lorenz, J.-O. Joswig, V. Lesnyak, S. Recknagel, N. Gaponik, U. Resch-Genger, and A. Eychmüller, *Dalton Trans.*, 2013, **42**, 12733–12740.

27. N. Lewinski, V. Colvin, and R. Drezek, *Small*, 2008, **4**, 26–49.

28. A. M. Smith, H. Duan, M. N. Rhyner, G. Ruan, and S. Nie, *Phys. Chem. Chem. Phys.*, 2006, **8**, 3895–3903.

29. E. Pöselt, S. Fischer, S. Foerster, and H. Weller, *Langmuir*, 2009, **25**, 13906–13913.

30. K. B. Subila, G. Kishore Kumar, S. M. Shivaprasad, and K. George Thomas, *J. Phys. Chem. Lett.*, 2013, **4**, 2774–2779.

31. H. Zhang, Z. Zhou, B. Yang, and M. Gao, *J. Phys. Chem. B*, 2003, **107**, 8–13.

32. L. Li, H. Qian, N. Fang, and J. Ren, *J. Lumin.*, 2006, **116**, 59–66.

33. Y. Zhang, L. Mi, P.-N. Wang, J. Ma, and J.-Y. Chen, *J. Lumin.*, 2008, **128**, 1948–1951.

34. V. Lesnyak, N. Gaponik, and A. Eychmüller, *Chem. Soc. Rev.*, 2013, **42**, 2905–2929.

35. Z. Fang, L. Liu, L. Xu, X. Yin, and X. Zhong, *Nanotechnology*, 2008, **19**, 235603.

36. H. Mattoussi, I. L. Medintz, A. R. Clapp, E. R. Goldman, J. K. Jaiswal, S. M. Simon, and J. M. Mauro, *JALA*, 2004, **9**, 28–32.

37. K. D. Mielenz, E. D. Cehelnik, and R. L. McKenzie, *J. Chem. Phys.*, 1976, **64**, 370–374.

38. C. Würth, M. Grabolle, J. Pauli, M. Spieles, and U. Resch-Genger, *Nat. Protoc.*, 2013, **8**, 1535–1550.

39. T. Felbeck, T. Behnke, K. Hoffmann, M. Grabolle, M. M. Lezhnina, U. H. Kynast, and U. Resch-Genger, *Langmuir*, 2013, **29**, 11489–11497.

40. G. Ellman, *Arch. Biochem. Biophys.*, 1959, **82**, 70–77.

41. P. K. Glasoe and F. A. Long, *J. Phys. Chem.*, 1960, **64**, 188–190.

42. A. E. Martell and R. M. Smith, *Critical Stability Constants, Vol. 5*, Plenum Press, New York, 1982.

43. P. D. Oram, X. Fang, Q. Fernando, P. Letkeman, and D. Letkeman, *Chem. Res. Toxicol.*, 1996, **9**, 709–712.

44. A. L. Rogach, *Mater. Sci. Eng., B*, 2000, **69-70**, 435–440.

45. N. Gaponik, D. V. Talapin, A. L. Rogach, K. Hoppe, E. V. Shevchenko, A. Kornowski, A. Eychmüller, and H. Weller, *J. Phys. Chem. B*, 2002, **106**, 7177–7185.

46. D. V. Talapin, A. L. Rogach, M. Haase, and H. Weller, *J. Phys. Chem. B*, 2001, **105**, 12278–12285.

47. D. V. Talapin, A. L. Rogach, E. V Shevchenko, A. Kornowski, M. Haase, and H. Weller, *J. Am. Chem. Soc.*, 2002, **124**, 5782–5790.

48. S. V. Kershaw, M. Burt, M. Harrison, A. Rogach, H. Weller, and A. Eychmüller, *Appl. Phys. Lett.*, 1999, **75**, 1694–1696.

